Surface Chemistry Guides the Orientations of Adhering E. coli Cells Captured from Flow

Zhou Xu, Wuqi Amy Niu, Sylvia L. Rivera, Mark T. Tuominen, M. Sloan Siegrist, and Maria M. Santore^{2,4*}

- 1. Department of Physics, University of Massachusetts, Amherst, MA 01003
- 2. Department of Polymer Science and Engineering, University of Massachusetts Amherst, MA 01003
- 3. Department of Microbiology, University of Massachusetts Amherst, MA 01003
- 4. Molecular and Cellular Biology Graduate Program, University of Massachusetts,

Amherst, MA 01003

*corresponding author: Maria Santore

Department of Polymer Science and Engineering

University of Massachusetts

120 Governors Drive Amherst, MA 01003

413-577-1417

santore@mail.pse.umass.edu

Abstract

Motivated by observations of cell orientation at biofilm-substrate interfaces and reports that cell orientation and adhesion play important roles in biofilm evolution and function, we investigated the influence of surface chemistry on the orientation of Escherichia coli (E. coli) cells captured from flow onto surfaces that were cationic, hydrophobic, or anionic. We characterized the initial orientations of non-motile cells captured from gentle shear relative to the surface- and the flowdirections. The broad distribution of captured cell orientations observed on cationic surfaces suggests that rapid electrostatic attractions of cells to oppositely charged surfaces preserves the instantaneous orientations of cells as they rotate in the near-surface shearing flow. By contrast, on hydrophobic and anionic surfaces, cells were oriented slightly more in the plane of the surface and in the flow direction compared with on the cationic surface. This suggests slower development of adhesion at hydrophobic and anionic surfaces, allowing cells to tip towards the surface as they adhere. Once cells were captured, flow was increased 20-fold. Cells did not reorient substantially on the cationic surface, suggesting strong cell-surface bonding. By contrast on hydrophobic and anionic surfaces, increased shear forced cells to tip toward the surface and align in the flow direction, a process that was reversible upon reducing the shear. These findings suggest mechanisms by which surface chemistry may play a role in the evolving structure and function of microbial communities.

Key words: microcolony, biofilm morphology, adhesion, electrostatic, cell capture

Introduction

The growth of a biofilm begins with the adhesion of individual bacterial cells to a device or tissue surface. Each adherent cell can then divide on a timescale of hours, its progeny forming a living community. It is now appreciated that, rather than a random mass of cells, biofilms possess shape and organization that develop in ways that reflect the local environment. This organization is evident early in biofilm growth, for instance in microcolonies containing as few as 100 cells, in a first layer on a surface. Microcolony organization and shape play key roles in further biofilm function, Potentially related to the spread of infection, antibiotic resistance, and the infiltration of confined spaces by biofilms. Surface interactions and their coupling to external factors guide biofilm growth, and are therefore of prime importance.

The impact of surface chemistry on infection and biofilms has been studied predominantly from a biomaterial perspective with the aim of developing resistant coatings. Surfaces that allow bacterial adhesion are found to support infection and therefore surface chemistries that avoid cell capture or retention are sought.^{11, 12} There has been limited effort to quantitatively distinguish characteristics of biofilms on surfaces of different bacteria-adhesive chemistries, ¹³⁻¹⁵ and we are far from a general understanding. Studies have determined that adhesive interactions can originate with pili ¹⁶⁻¹⁸ and flagella, ¹⁹⁻²² and these appendages further influence the motions of adhered bacteria such as twitching and rotating. ^{20, 23} Adhesive interactions involving the cell body with a surface are thought, at least in some cases, to be stronger than the adhesion via appendages. ²² Indeed, capsular bacteria present a "polar" spatial distribution of adhesion molecules over their surfaces such that the ends of *Escherichia coli* or *Pseudomonas aeruginosa* are more adhesive than the sides. ²⁴⁻²⁷

In some biofilms, for instance those involving rod-shaped cells, the cells growing in contact with the surface exhibit substantial order, orientation, and transitions in orientation that further predispose key aspects of biofilm character. The ability of cells to reconfigure on a surface is thought to result, at least for some substrates, from stresses developed within and between growing cells relative to the strength of surface adhesion. These studies of colony morphogenesis typically employ cells initially lying flat on a surface, for instance sandwiched at an agar / glass interface.

In natural environments cells are often captured on surfaces from flow^{32, 33} or settling under gravity.^{34, 35} The capture process, combined with surface chemistry, may introduce a variety of initial cell configurations on a surface. For instance, the vorticity of shear flow causes cells to rotate as they travel along the surface,³⁶ potentially creating a variety of cell orientations at the moment of first surface encounter. The forces of rotation, the strength of the initial adhesion at the sub-second timescale of first contact, and the ability of the initially formed bonds to adjust in the moments of capture are all factors that potentially influence the initial cell orientation. Cells captured in the resulting variety of initial configurations may ultimately evolve differently into biofilms compared with cell populations where all the cells are initially flat to a surface.

In this work we probe the impact of surface chemistry on the orientation of cells captured from flow for a flagella-free *E. coli* strain, focusing on model surfaces with cationic, hydrophobic, and anionic functionality, and further addressing the stability of the adhered cells to increased shear. We note that wild-type strains can be irregular in their flagella expression, sometimes/often not

expressing flagellae.³⁷ Therefore studies such as the current work that focus on cell-body surface interactions are broadly relevant. To distinguish the impact of flow and chemistry from a settling-type behavior where cells accumulate on a surface driven by gravitational forces (the focus of a separate study), we employ a slit-shear cell whose walls are oriented perpendicular to the floor in the current work. Results are interpreted in the context of distributions of orientation relative to the surface plane and to the flow direct and benchmarked against rod-shaped particles of similar size as the *E. coli* bacterium.

Materials and Methods

Bacterial Cultivation and Characterization. E. coli strain JW1881 was purchased from the Coli Genetic Stock Center (New Haven, CT). This strain is a genetic knockout of the *flhD* gene, which encodes a transcriptional regulator of flagellar gene expression. The lack of flagella was confirmed via electron microscopy and the lack of motility was confirmed in motility plate assays. ³⁷ E. coli were grown overnight at 37°C in lysogeny broth (LB). After 16 h growth, bacteria were back-diluted 1:50 in LB, incubated at 37°C for 2 h, and harvested in log phase. To remove residual proteins and other macromolecular constituents, cells were washed three times with phosphate-buffered saline (PBS, 0.008M Na₂HPO₄, 0.002M KH₂PO₄, and 0.15 M NaCl) before resuspending in PBS. For all bacteria flow experiments, the re-suspended cells (10⁸ cells/ml) were used within 1 h of preparation. Viability screening with propidium iodide (Sigma-Aldrich, excitation/emission at 535 nm/ 617 nm) before and after flow experiments confirmed that the bacteria maintained viability throughout all experimental procedures. Drops of the E. coli suspension were imaged at 100x in phase contrast and analyzed via Oufti³⁸ using the cell detection analysis tool to determine the length and width of each cell. From 350 to 400 cells analyzed for each of three suspensions grown on separate days, statistics were generated for the average length and widths of cells and the standard deviations on those quantities.

<u>Engineered Surfaces</u>. Engineered surfaces were made using microscope slides (Fisher finest) that had been soaked overnight in concentrated sulfuric acid and then rinsed thoroughly with deionized water and dried under nitrogen. These slides were then used directly and immediately as the anionic surface. Hydrophobic surfaces produced by applying a coating of C16:

hexadecyltrichlorosilane, 95% from Gelest. The dry acid etched slides were balanced on a petri dish containing the chlorosilane inside a dessicator that was then held under vacuum for 30 minutes. The slides were used the same day. The advancing contact angle was consistently between 104° and 106°. Cationic surfaces were produced *in situ* in the flow chamber, prior to bacteria studies. After sealing an acid etched slide in the chamber, it was filled with flowing PBS. A 100 ppm solution of poly-L-lysine hydrobromide (PLL, from Sigma Aldrich, 15,000-30,000 g/mol nominal molecular weight) was flowed through the chamber at a wall shear rate of 5 s⁻¹ for 10 minutes, more than sufficient to saturate the surface, and then flowing buffer was returned to the chamber. We previously demonstrated that this procedure produces an adsorbed layer of PLL of about 0.4 mg/m², which is flat (within a few nm of the surface),³⁹ and is not removed, in the time frame of a few hours, upon exposure to buffer of a variety of ionic strengths;^{40, 41} flowing micro or nanoparticles;⁴² a variety of negatively charged proteins, mammalian cells.⁴³ or bacteria such as *Staphylococcus aureus*.⁴⁴

<u>Bacteria Capture Studies</u>. In studies of bacteria capture, test surfaces comprised one wall of a laminar slit flow chamber. After the chamber was sealed PBS was introduced. The acid etched and hydrophobic surfaces were employed directly while the cationic surfaces were made *in situ* through deposition of PLL and re-introduction of PBS described above. The chamber was then fitted into a custom-built lateral optical microscope with a 20x Nikon objective and the test surface oriented perpendicular to an optical bench so that gravity did not act normal to the surface, illustrated in Figure 1. After flowing PBS, video recording was initiated and *E. coli* in PBS were flowed through the chamber at a concentration of 10⁸ cells/ml. In most studies the wall shear rate was 5 s⁻¹ though some studies at 25 s⁻¹ were conducted, as mentioned. After 30

minutes of flowing E. coli suspension, flowing PBS at 5 s⁻¹ was reintroduced to flush away free cells. The dynamic portion of the run was recorded at 20x to quantify cell accumulation in a large field. The chamber was moved slightly to 3 positions near the center of the channel and images were captured using a 40x Nikon objective for later analysis of cell orientation. The flow rate was then increased to $110 \, \text{s}^{-1}$ and the same 3 regions were imaged. Then the flow rate was set back to $5 \, \text{s}^{-1}$ and the same regions of the surface imaged again at 40x.

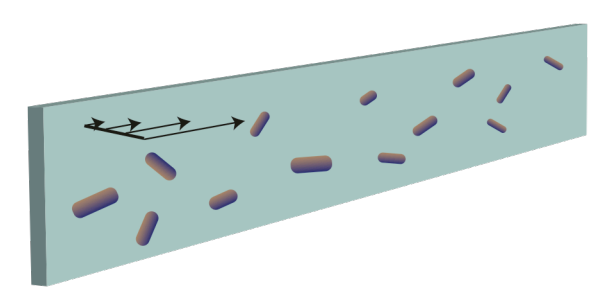


Figure 1. Schematic of the functionalized wall orientation of flow chamber, viewed from within the solution, at perspective, looking towards the surface and showing velocity gradient in perspective. The variety of cell orientations is meant to reflect a moment in time, with many of the cells freely moving. From the viewing angle and perspective in solution towards the surface, it is not possible to indicate which cells are in flow and which are in contact with the surface.

Images were analyzed by first background-subtracting a control frame prior to bacteria introduction, to remove image features from aberrations on the camera's detector array. Then each cell was located in the frame of interest employ a self-written Python code implementing the OpenCV library. The vertical orientation of each cell was classified by human eye based on its shape (round-like: standing; rod-like: tipped; other: leaning). When a cell was identified as tipped, its shape was fit to an ellipse to determine its major axis. The cell angle was found by calculating the angle between the major axis and the horizontal (flow) direction.

Data were measured on 3 of each type of surface, employing bacteria prepared separately on different days. The resulting data sets facilitated analysis for more than 700 cells on each surface type. Unpaired T tests (with equal variances) were conducted in Excel on the average orientations of the cells on the different surfaces, to determine the significance of the reported orientations.

Results and Discussion

Cell Characterization

E. coli suspensions were imaged by phase contrast at 100x to determine bacterial cell length and width. Using three separate suspensions grown on different days and 350-400 cells from each, the average cell length was determined to be 3.0 ± 0.3 μm and the average cell width was 0.96 ± 0.05 μm. These dimensions fall within the expected range for log phase growth.

Cell suspensions contained fewer than 2% dead cells, as determined by propidium iodide staining. In the studies below, cells captured on all the surfaces were also alive, with less than 2% dead cells in the captured populations.

Initial Cell Capture

In studies of cell orientation, cells were captured from shear flow onto test surfaces at a wall shear rate of 5 s⁻¹. Cationic surfaces were comprised of a saturated layer of physisorbed poly-L-lysine (PLL) that was bound irreversibly on the time scales and under the conditions of this study. C16-monolayers comprised the hydrophobic surfaces; the anionic surfaces were the silica surfaces of acid-etched microscope slides. The vertical orientations of the test surfaces in the flow chamber avoided the influence of gravity to drive cells towards or away from the surfaces.

In Figure 2, following buffer flow, cell capture proceeded shortly after the flowing cell suspension was introduced. On all three surface types, the numbers of captured cells increased linearly with time but the rate of cell accumulation depended on surface chemistry. Cell capture was highly reproducible as 3 separate runs, using bacteria prepared separately on different days,

and superimposed for each surface chemistry. Also on all three surfaces, captured cells were seen to be immobilized and did not release from the surface when flowing buffer was later introduced. The most rapid accumulation was seen on the cationic surface and the least rapid accumulation on the anionic surface. Cell capture was terminated by reintroduction of flowing buffer at 5 s⁻¹ after 30 minutes of bacteria flow. The fixed 10-minute cell flow times for all runs ensured that the ages of the cell-surface contacts were held constant over the course of this study.

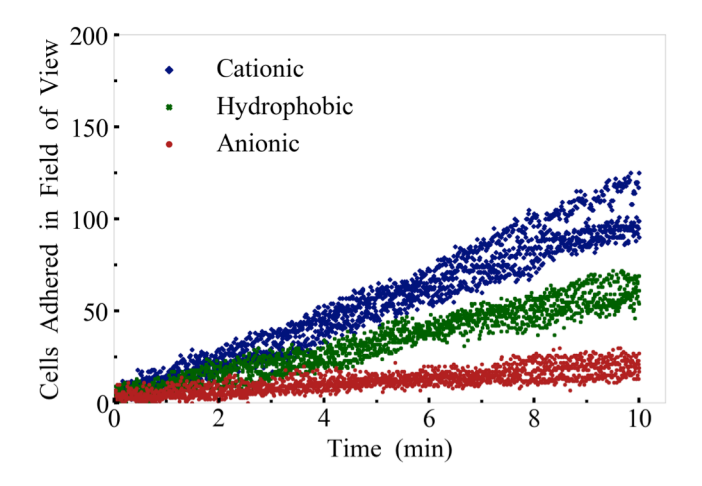


Figure 2. Cell accumulation from flowing suspensions containing $\sim 10^8$ cells/ml onto surfaces of different chemistries. The field of view is 276 μ m x 180 μ m. The wall shear rate is 5 s⁻¹.

The slopes of the cell capture plots in Figure 2 represent cell accumulation rates. The observed accumulation rates on the cationic surfaces are in good agreement with calculations for the transport-limited capture of rod-shaped particles and with the observed capture of silica rod microparticles having a size and aspect ratio close to that of the *E. coli* cells. ⁴⁹ This is the maximum observable capture rate, suggesting that processes involved in capturing and the initial holding of cells occur more quickly than cell arrival to the interface by diffusion/convection.

While the cell capture on cationic surface in Figure 2 was conducted at a wall shear rate of 5 s⁻¹, separate runs confirmed transport-limited capture at higher wall shear rates, up to at least 25 s⁻¹. By contrast, it was found that at 25 s⁻¹ there was negligible capture of *E. coli* on hydrophobic surfaces. Thus, a more gentle shear of 5 s⁻¹ was employed here for all surfaces, in Figure 2.

A key point illustrated in Figure 2 is that, different from the rapid transport-limited capture on the cationic surfaces, $E.\ coli$ cells are captured considerably more slowly on anionic and hydrophobic surfaces. This indicates that interfacial processes critical to cell capture on hydrophobic and anionic surfaces occur more slowly than the transport of cells to the surfaces. This might be expected since $E.\ coli$ cells are negatively charged and experience nanometer scale attractions (κ^{-1} = 1 nm in PBS) towards the cationic surfaces. In the absence of a steric or other barrier that is longer range, the electrostatic attractions may dominate as a cell first approaches a cationic surface and could be sufficient for capture. By contrast the electrostatic repulsions between the cells and the anionic surfaces may present a nanometer scale repulsive barrier that must be overcome by other attractive interactions (for instance hydrogen bonding) in order for negatively charged $E.\ coli$ cells to be captured. The reasons for the relative slowness of capture at hydrophobic surfaces is less clear but the slower capture rate in Figure 2 is notable.

While cells are not captured at all on hydrophobic surfaces at wall shear rates as high as 25 s⁻¹, once cells have adhered to the hydrophobic surface for a few minutes at 5 s⁻¹, they are retained even when the wall shear rate is increased to 110 s⁻¹ in the shear challenge studies below. The inability to capture cells on hydrophobic surfaces at a modest shear rate of 25 s⁻¹ combined with the inability to remove cells from the same surfaces at higher shears emphasizes that the

observed accumulation rate is not a direct measure of adhesive strength. The ability to capture cells at given conditions reflects the kinetics of the particular capture process, while separate mechanisms leading to cell detachment depend, at least in part, on the tightness of binding which may be influenced by factors other than those critical for initial capture.

Initial Orientation

Upon introduction of flowing buffer at 5 s⁻¹ after cell capture, three images of retained cells were immediately acquired, at nearby positions on each slide. Only three images were obtained because this enabled us to recognize the positions of the various cells and return quickly to these surface regions at later times, to determine the fates of each cell. Taking more images would take more time, potentially allowing undesired relaxation of orientations between the first and last images on a slide. At least three specimens of each surface type were studied in this fashion.

Figure 3 illustrates how cells were classified as "standing" "leaning" or "tipped". Cells were classified as "standing" when, from the perspective of the microscope, the cell appeared mostly as a dot. These cells were perpendicular to the surface within a precision of about 15 degrees. "Leaning" means that the rod shape of the cell was barely evident in the micrograph but the aspect ratio or length was smaller than that of other cells or the 3 µm length in characterization studies. We estimate that the leaning category includes cells that were adhered by their ends, having angles in the approximate range 15-70 degrees from the normal to the surface. The final category, "tipped," describes cells that appeared mostly in plane, with the largest aspect ratios. We are careful to choose the term "tipped" rather than "side-on" or other language implying that the side of the cell was in contact with the surface, since contact was not measured. It is

conceivable that cells could be substantially tipped and still only adhered at one end. Even so, in the tipped configuration, captured cells possess a greater excluded surface area (blocking other cells from accessing the surface) compared with cells in the leaning or standing configuration.

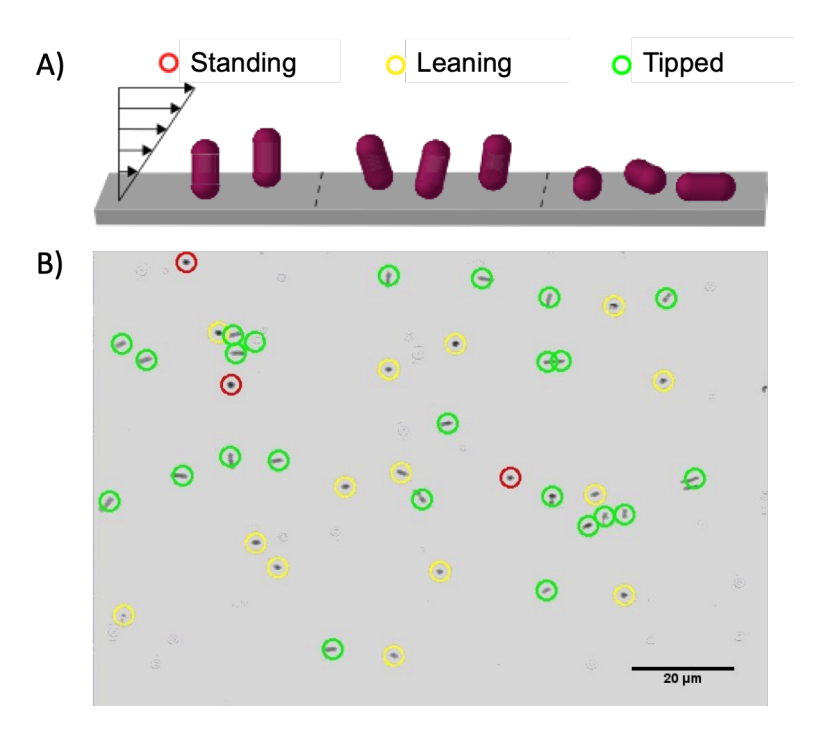


Figure 3. (A) Diagram and (B) examples of cells that are standing (red circles), leaning (yellow circles), and tipped (green circles). The marks that on the image that are not circled are on the detector and not bacterial cells.

Figure 4, summarizing the orientation of cells captured on the three surface types reveals a statistically significant impact (p < 0.01, T-test) of surface chemistry on whether cells captured at 5 s⁻¹ were standing, leaning, or tipped. On the cationic surface, cells were captured in proportions that might be expected: The fraction of cells "standing" is relatively small because

modest deviations of cell orientations from perpendicular can be readily discerned, and those cells would be classified as leaning. Within a random distribution of orientations, only a small fraction would be classified as "standing," while most will be leaning or tipped. While some difference between leaning and tipped may be a matter of perspective, we found that two researchers in a blind exercise, when given the definitions of standing, leaning and tipped, agreed on the classifications of cells for 95% of the cells on a PLL surface, with all the discrepancies falling between leaning and tipped. Thus while the exact characterizations of cell orientation may vary slightly by researcher, there are clear differences, which turn out to be statistically significant, in the orientations of populations of cells on the different surfaces. Most notably our analysis reveals a statically significant (p < 0.01, T-test) greater proportion of cells captured on the hydrophobic surface are "tipped" compared with the cells on the cationic or anionic surfaces. There are also fewer cells leaning on the hydrophobic surface compared with the other surface types. Thus on the hydrophobic surface, there is a smaller tendency for cells to protrude into the flow compared with the charged surfaces. While we cannot say that the cell-surface contact is greater on the hydrophobic surface, the cells are more "pushed over" compared on the cationic surface. The cells captured on the anionic surface also exhibit a lower protrusion into solution compared with cells on the cationic surface, though they are statistically different from the cells on the hydrophobic surface which are more pushed over still.

In addition to the orientation of cells relative to the surface after initial capture, the histograms of Figure 4 summarize the orientations of the tipped cells relative to the flow direction, with zero being perfect alignment. Our analysis revealed a small but statistically significant cell alignment relative to the flow direction (\pm 15 degrees) on the cationic surface at 5 s⁻¹, and slightly greater (p

< 0.01, T-test) alignment of cells favoring the flow direction on the hydrophobic and anionic (glass) surfaces.

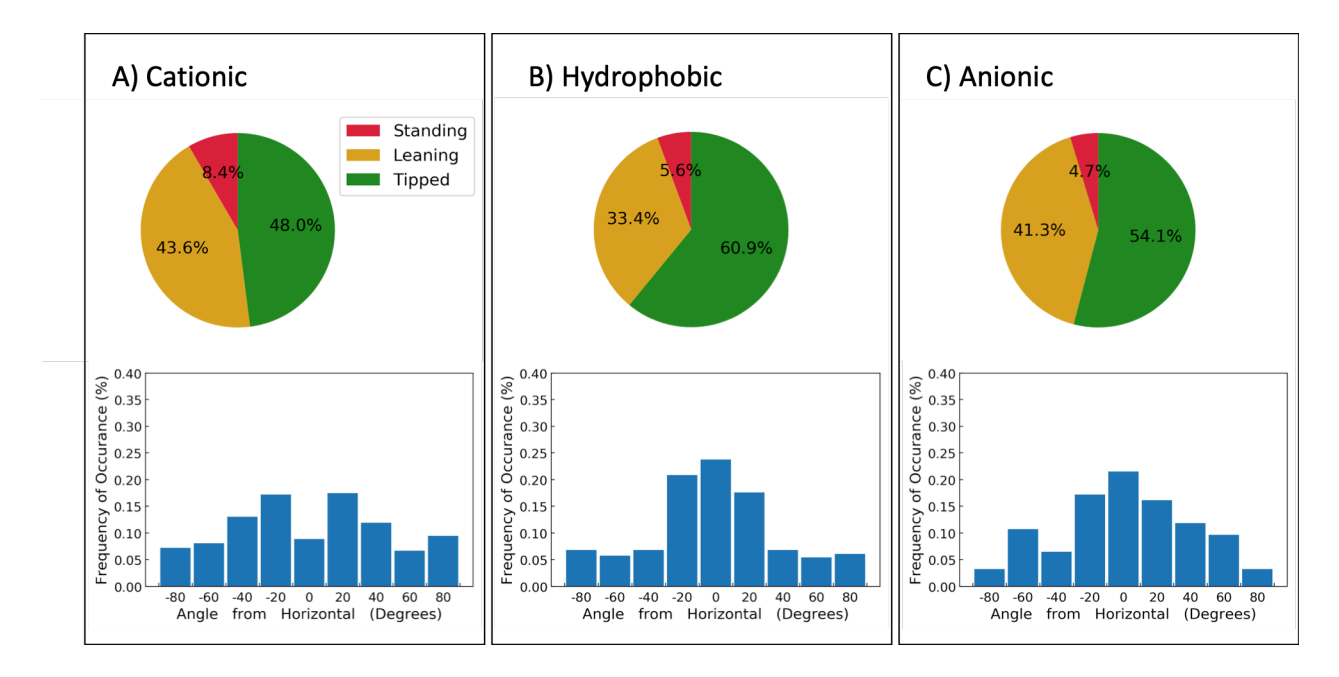


Figure 4. Orientation of *E. coli* on A) cationic, B) hydrophobic, and C) anionic glass surfaces after capture during shear flow at 5 s⁻¹. Pie charts show orientation relative to the surface while histograms indicate the orientation of tipped cells relative to the flow direction.

Shear Challenge

After capturing and imaging cells in flow at 5 s⁻¹, a process taking 30 minutes from start of adsorption, the flow was increased to 110 s⁻¹. Additional images were then recorded, within about a minute, for the same surface regions as before. Representative images for the cationic, hydrophobic, and anionic glass surfaces before and during the imposition of 110 s⁻¹ shear

challenge are shown in Figure 5. Cells identified as standing, leaning, and tipped are color-coded. First, it is clear that there is negligible cell escape at the elevated shear flow, even on the hydrophobic and glass surfaces. Next, because the same surface regions have been imaged in the examples for each surface type, changes in cell orientation are evident. For instance, on the cationic surface, not only are the cells originally classified as standing, leaning, or tipped retained in those conformations, the cell orientation is largely unchanged relative to the flow direction as well. By contrast on the anionic glass surface and to an even greater extent on the hydrophobic surface, an increase in shear from 5 to 110 s⁻¹ produces a change in cell orientation. The cells are pushed over somewhat, so that there are fewer cells standing at 110 s⁻¹ compared to 5 s⁻¹, and there is an increased proportion of tipped cells. Further, the cells on the anionic glass and hydrophobic surfaces become more aligned with the flow as the shear is increased.

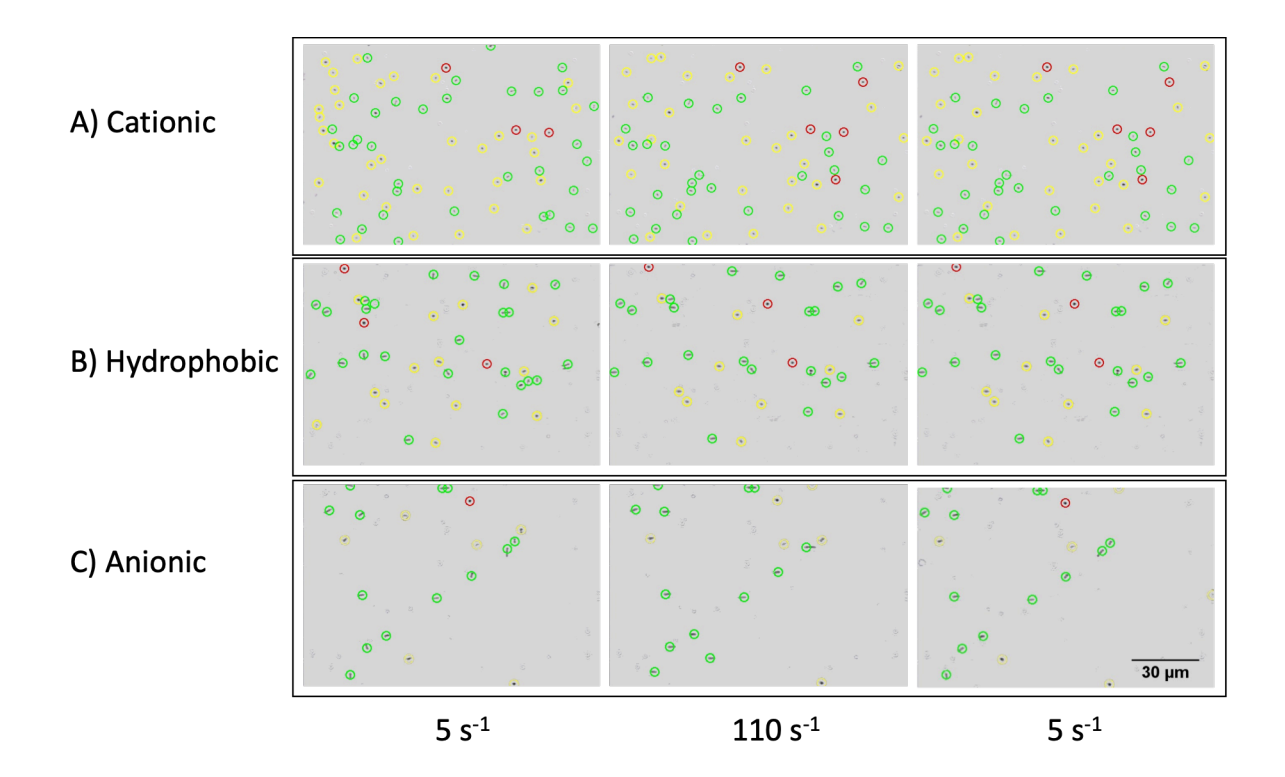


Figure 5. Example micrographs for A) cationic B) hydrophobic and C) anion surfaces, showing cells within 30 minutes of capture from a wall shear of 5 s⁻¹, during exposure to shear of 110 s⁻¹, and finally in right-most panels, 2 minutes after the shear has returned to 5 s⁻¹. The circles indicate how cells were classified as standing (red) leaning (yellow) or tipped (green), while the images themselves indicate alignment with shear in some cases.

The impact of increased shear is summarized in Figure 6. We found no statistically significant impact of increased shear on the orientations of cells on the cationic surface. In contrast, increasing the flow to $110 \, \text{s}^{-1}$ tips the cells on the anionic and hydrophobic surfaces toward the

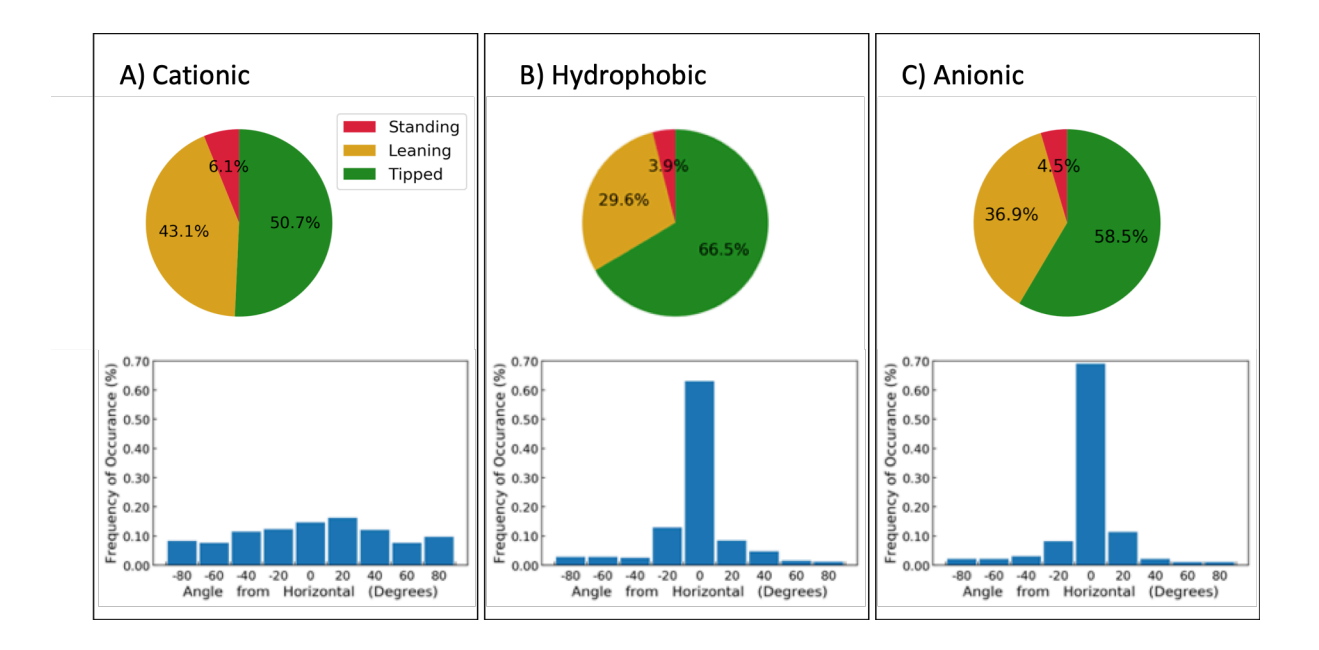


Figure 6. Orientation of *E. coli* on A) cationic, B) hydrophobic, and C) anionic glass surfaces shortly after increasing shear flow to 110 s⁻¹. Pie charts show orientation relative to the surface while histograms indicate the orientation of tipped cells relative to the flow direction.

surface and aligns them in the direction of flow.

Relaxation

After the cells had been exposed to a shear rate of $110 \, \text{s}^{-1}$ for about two minutes, the flow was reduced back to $5 \, \text{s}^{-1}$, and images of the same regions of the surface were obtained a few minutes later to determine the extent to which alignment was reversible. On the glass and hydrophobic surfaces, flow had tipped cells away from the vertical; however, upon return to weaker shear flow at $5 \, \text{s}^{-1}$, cells did not fully recover to their original angles relative to the surface, and stayed

slightly preferentially in a leaning configuration on the frame of minutes. However, following reduction of the flow, cells were found to randomize their orientations with respect to the flow direction though the original angular distribution was not attained at the short times studied. These observations suggest that reorientations driven by flow tend not to be maintained by the same type of bonding involved in cell capture, even though the exposure time at high shear would be sufficient for bonds, like those involved in capture, to develop.

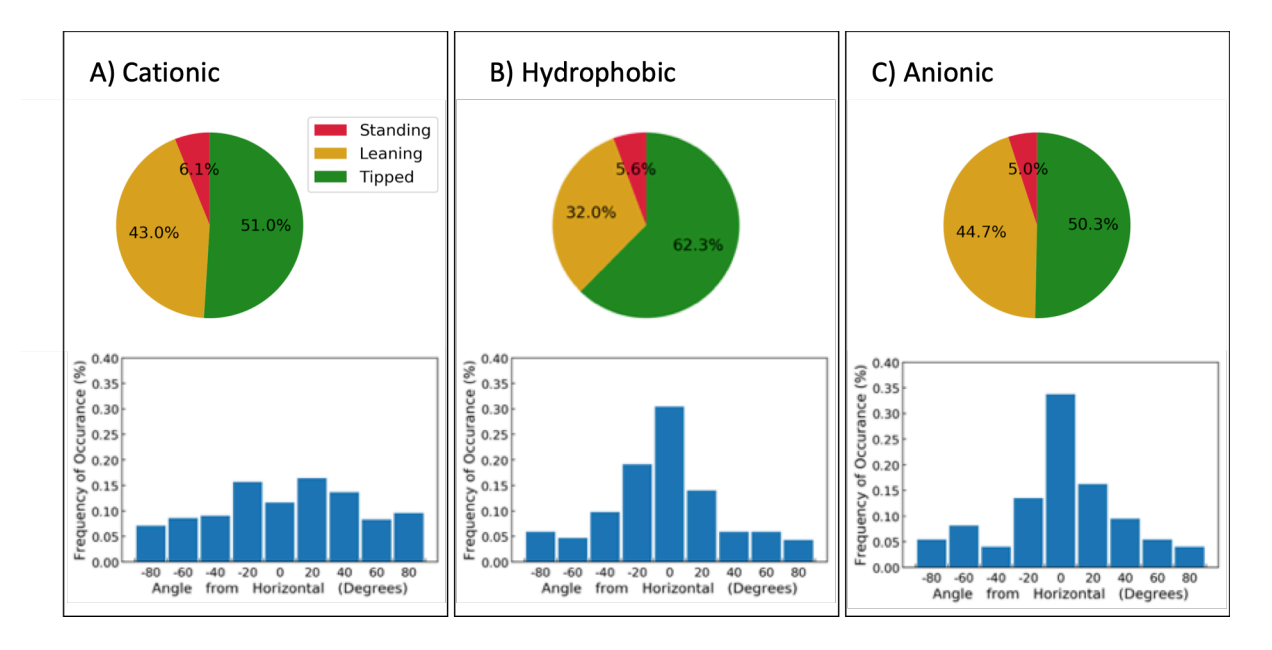


Figure 7. Orientation of *E. coli* on A) cationic, B) hydrophobic, and C) anionic glass surfaces 2 minutes after returning to gentle shear flow at 5 s⁻¹. Pie charts show orientation relative to the surface while histograms indicate the orientation of tipped cells relative to the flow direction.

Shear and Cell Rotation

Figure 8 schematically summarizes how surface chemistry and flow influence the orientation of *E. coli* captured on a surface from flow.

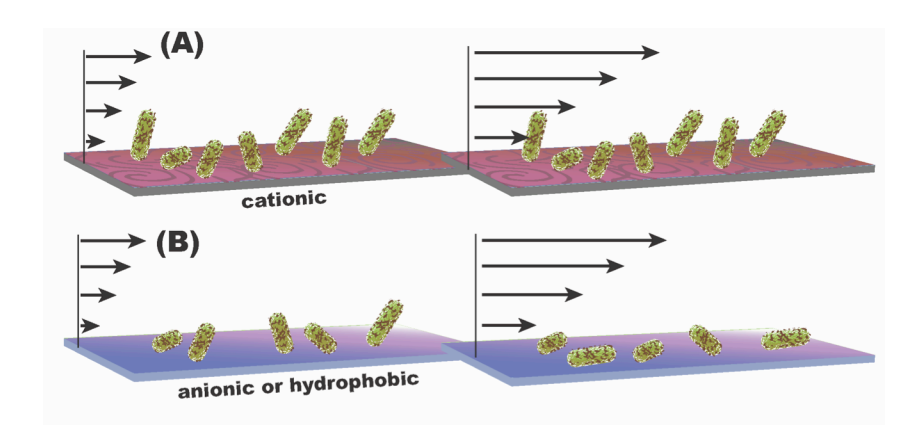


Figure 8. Summary schematic of the influence of surface interactions and flow on the orientation of captured cells. In (A) on a cationic surface, the distribution of captured cell orientations includes those that are tipped only slightly relative to the surface normal. When the flow is increased, the cells on the cationic surface are mostly unperturbed. On hydrophobic or anionic surfaces in (B), the distribution of initially captured cells includes more orientations that are further tipped over from the surface normal. Then when the flow is increased, the cells lean over towards the surface even more.

The initial distribution of orientations of captured cells is explained, in part, by the tumbling motions or "Jeffrey orbits" undergone by ellipsoids in shearing flow prior to adhesion.

Depending on the orientation of the cell relative to the shear direction, flowing cells can undergo cartwheel or log rolling rotations, or motions in between. Thus cells sample a variety of orientations relative to the flow direction and the surfaces, as they diffuse towards the surface and travel along it prior to capture. Flagella-free *E. coli* have been shown to quantitatively follow the predicted frequencies of Jeffrey orbits, including a reduced rotation frequency as cells approach a surface.³⁶

The transport-limited capture of E. coli on the cationic surface in Figure 2 indicates that the underlying adhesion kinetics, driven by electrostatic attractions, are rapid. Thus cells may become trapped in the orientation occurring at the moment of a surface encounter. Notably, transport limited capture of spherical microparticles carrying negative surface charge^{51, 52} has been observed on cationic surfaces for shear rates up to 800 s⁻¹ and at least 15 s⁻¹ for negatively charged silica rods microparticles⁴⁹ supporting the possibility that capture driven by electrostatic attractions is rapid. The distributions of standing, leaning, and tipped configurations reported here for E. coli are similar to those in a previous study of negatively charged silica rod-shaped particles of similar size and aspect ratio. ⁴⁹ That previous study with silica rod-shaped particles also reported a similar angular distribution relative to the flow direction as we report here for E. coli. Thus, the rapid and irreversible bonding of particles with an oppositely charged surface appears to lead to similar approximate particle orientation distributions. Further the rod shaped silica particles, like the E. coli studied here on the cationic surface, did not reconfigure when flow was increased to 110 s⁻¹. Also, while E. coli are known to adhere by their poles as a result of adhesion molecules on the ends of the cells, $^{24-27}$ the similarities between the behavior of E. coli and negatively charged silica rods of the same size and shape suggests that non-specific electrostatic attractions, rather than particular surface proteins, are responsible for the observed behaviors.

The observed tendency for capture on a cationic surface to "lock in" the instantaneous orientation of *E. coli* cells encountering a surface provides a point of contrast for the same cells on hydrophobic and anionic surfaces. Even at gentle flows of 5 s⁻¹, cells on hydrophobic and anionic surfaces appear more aligned with the surface and the flow compared the configurations

on the cationic surfaces. This suggests that on the hydrophobic and anionic surfaces, the

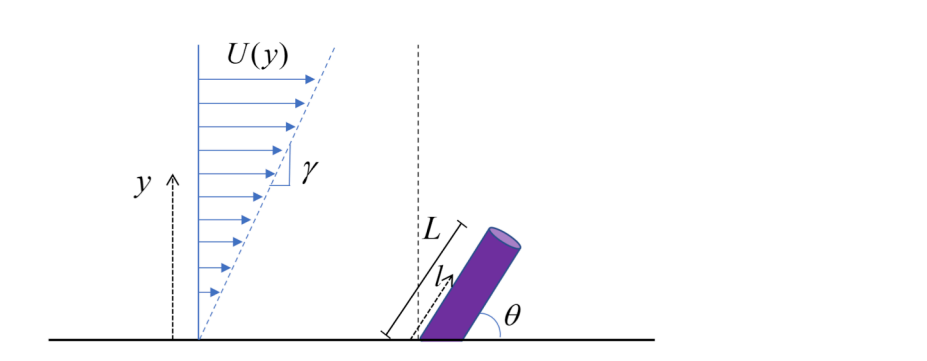


Figure 9. Schematic of adhered cell of length L, showing tilt angle relative to the surface, and length l along the cell.

times
cales
for
initia

re are

captu

more

nearl

y similar to the timescale of cell rotation in flow. Here the rotational period⁵⁰ of \sim 3 s for a cell with an aspect ratio of 2.5 and a wall shear rate of 5 s⁻¹ suggests a capture time on the order of 0.1 s to rotate a fraction of turn. As cells encounter a surface and start to be captured, they rotate down towards the surface and align slightly in the flow direction at the same time as adhesion strength grows stronger, producing fewer standing cells even at low flow rates. Further the overall adhesion on the hydrophobic and anionic surface may be weaker than on the cationic surface, as cells on the hydrophobic and anionic surfaces can be manipulated by increases in shear applied minutes after initial capture. On cationic surfaces, *E. coli* and the previously studied silica rod microparticles resisted reorientation in increased shear up to 110 s⁻¹.

The observation that increased flow is able to orient cells on hydrophobic and anionic surfaces but not on cationic surfaces motivates calculations of the force and torques imposed by shear on adherent cells. Modeling cells of length L and radius r, adhered by one end and tipped at angle θ

relative to the surface in Figure 9, the integrated force and torque was calculated, as detailed in supporting information. The calculations employed a drag coefficient for laminar flow across an elliptical cylinder, ⁵³ which is the effective shape, in the direction of flow, for the cross section of a tilted, end-adsorbed bacterial cell. In shear, the tip of the cell experiences stronger flow than the part nearest the surface, and so force and torque were integrated up the length of the cell to account for variations in flow over its length, giving:

$$F = \frac{\pi \mu^3}{2r^2 \rho^2 \gamma} \int_0^{R_e(L)} \frac{R_e}{S} dR_e$$
 (1)

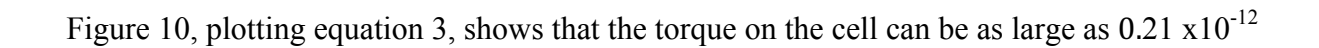
$$\tau = \frac{\pi \mu^4}{4r^3 \rho^3 \gamma^2} \int_0^{R_e(L)} \frac{R_e^2}{S} dR_e \tag{2}$$

where

$$S = \frac{1}{2} \left(1 + \sigma \right) - c - \ln \left(\frac{R_e}{8(1+\sigma)} \right) \tag{3}$$

and where $\sigma = \frac{1-\sin\theta}{1+\sin\theta}$ and c = 0.57721 (Euler's constant.)

Here the particle Reynolds, R_e , number is defined $R_e = \frac{2rU\rho}{\mu}$, with ρ and μ the fluid density and viscosity, respectively. Notably, the velocity U, and hence the Reynolds number, varies linearly from zero up the length of the cell, allowing the integration to be developed employing R_e as the integration variable. For cells of length L=3 µm, and radius 0.5 µm, the Reynolds number at the free tip of the cell reaches 1.5 x 10^{-5} when the cell is oriented vertically and it approaches zero as the cell's orientation becomes increasingly flat to the surface.



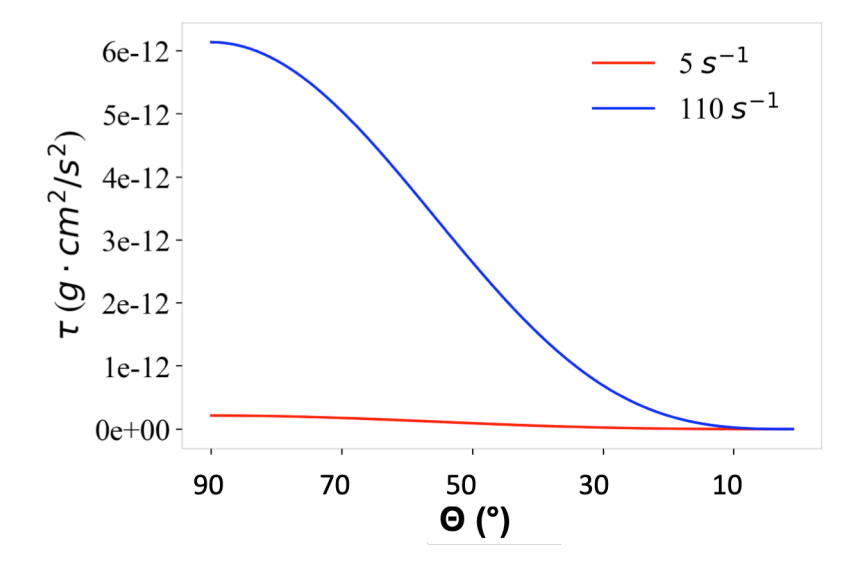


Figure 10. Decrease of torque as the tilt angle increases, bringing a cell closer to the surface. Calculation is for a cell, 3 μ m long and 1 μ m in diameter that is aligned in the flow direction as its angle increases such that it tips more towards the surface.

g*cm²/s² at 5 s⁻¹, and 6.1 x 10^{-12} g*cm²/s² at 110 s⁻¹. As the cell angle θ is rotated towards the surface, the torque on the cell is reduced. While this explains the tendency of cells to rotate towards the surface, it is also evident that the torque diminishes as a cell becomes increasingly tipped. The observation that cells tip in flow on the glass and hydrophobic surfaces is further consistent with the calculated maximum force of 3 x 10^{-8} g cm/s² or 0.3 pN parallel to the surface for cells in the vertical configuration and a wall shear rate of 110 s⁻¹. This lateral force is substantially less than the 0.3-0.9 nN forces measured by AFM to remove *E. coli* from glass. Thus cells tend to tip in flow on glass and hydrophobic surfaces on the surface without being removed. The substantial reduction in torque in Figure 10 with rotation angle further suggests that flow may not push cells into extensive contact with the surface.

Even without surface contact along the full length of the cell, however, a more tipped cell configuration can prevent cells in solution from reaching the surface and potentially influence the arrangements of daughter cells through excluded area interactions. Conversely, one might imagine that surface forces could drive further cell adhesion in a wetting type mechanism, in some situations. Hence tipping of cells by shear forces produces multiple potential routes for surfaces to influence evolving colony morphology.

Conclusions

This work demonstrated that, while shear tends to align *E. coli* cells during and after the process of surface capture, the extent of alignment depends on surface chemistry, as summarized schematically in Figure 8. For surfaces of fundamentally different chemistries (anionic, cationic, hydrophobic), the rates of cell accumulation from gentle shearing flow (5 s⁻¹) correlate with the orientation of the initially captured cells, with more alignment on the slower binding surfaces. For instance, cells were found to be captured on cationic PLL layers at a rate limited by diffusion, which indicated rapid development of adhesive contact. In this case a distribution of cell orientations reflected cell rotation in free flow near the surface prior to capture, suggesting cells were trapped in their instantaneous orientations at the moment of initial surface contact. By contrast, on the hydrophobic and anionic surfaces, a cell accumulation of less than 25% of the transport limited rate suggested slower development of adhesion upon cell-surface contact. Here the captured configurations of the cells were more tilted towards the surface and aligned with the

flow. This suggests the cells continued to rotate progressively with the flow during the process of adhesive capture.

Separate from processes influenced by capture rate, the binding strength or ability to slip at the cell-surface contact region was also found to be important. On the cationic surfaces, the insensitivity of the cell configurations to increased shear evidenced strong cell binding, able to withstand torques of 6 x 10⁻¹² g cm²/s². The immobility *E. coli* on the cationic surface, where cells did not tilt or align when flow was increased, was similar to behaviors observed with negatively charged silica micro-rods adhering to the same cationic surfaces. This suggests electrostatic attractions produce relatively strong adhesion that is also resistant to slippage at the point of contact. By contrast, *E. coli* on hydrophobic and anionic surfaces aligned with shear, a process that was partially reversible on the timescale of several minutes. The cell reconfiguration suggests slippage in the region of cell-surface contact, while cells were retained on the surface. With cell orientation on a surface now understood to influence biofilm structure and cell function within a bacterial community, ³⁰ the current findings demonstrate how surface chemistry and shear couple to influence biofilm development.

Acknowledgements This work was supported by NSF CBET 1848065.

Supporting Information:

- Shear Force and Torque on an Adherent E. coli Cell Treated as a Rod

References

- 1. Branda, S. S.; Vik, A.; Friedman, L.; Kolter, R. Biofilms: the matrix revisited. *Trends Microbiol.* **2005**, *13*, 20-26.
- 2. Kirketerp-Moller, K.; Jensen, P. O.; Fazli, M.; Madsen, K. G.; Pedersen, J.; Moser, C.; Tolker-Nielsen, T.; Hoiby, N.; Givskov, M.; Bjarnsholt, T. Distribution, organization, and ecology of bacteria in chronic wounds. *J. Clin. Microbiol.* **2008**, *46*, 2717-2722.
- 3. Swidsinski, A.; Weber, J.; Loening-Baucke, V.; Hale, L. P.; Lochs, H. Spatial organization and composition of the mucosal flora in patients with inflammatory bowel disease. *J. Clin. Microbiol.* **2005**, *43*, 3380-3389.
- 4. Wolfaardt, G. M.; Lawrence, J. R.; Robarts, R. D.; Caldwell, S. J.; Caldwell, D. E. Multicellular Organization in a Degradative Biofilm Community *Appl. Environ. Microbiol.* **1994**, *60*, 434-446.
- 5. Mamou, G.; Mohan, G. B. M.; Rouvinski, A.; Rosenberg, A.; Ben-Yehuda, S. Early Developmental Program Shapes Colony Morphology in Bacteria. *Cell Reports* **2016**, *14*, 1850-1857.
- 6. Beroz, F.; Yan, J.; Meir, Y.; Sabass, B.; Stone, H. A.; Bassler, B. L.; Wingreen, N. S. Verticalization of bacterial biofilms. *Nat. Phys.* **2018**, *14*, 954-+.
- 7. Flickinger, S. T.; Copeland, M. F.; Downes, E. M.; Braasch, A. T.; Tuson, H. H.; Eun, Y. J.; Weibel, D. B. Quorum Sensing between Pseudomonas aeruginosa Biofilms Accelerates Cell Growth. *J. Am. Chem. Soc.* **2011**, *133*, 5966-5975.
- 8. Enos-Berlage, J. L.; McCarter, L. L. Relation of capsular polysaccharide production and colonial cell organization to colony morphology in Vibrio parahaemolyticus. *J. Bacteriol.* **2000**, *182*, 5513-5520.
- 9. Lee, K. W. K.; Periasamy, S.; Mukherjee, M.; Xie, C.; Kjelleberg, S.; Rice, S. A. Biofilm development and enhanced stress resistance of a model, mixed-species community biofilm. *Isme J.* **2014**, *8*, 894-907.
- 10. Cho, H. J.; Jonsson, H.; Campbell, K.; Melke, P.; Williams, J. W.; Jedynak, B.; Stevens, A. M.; Groisman, A.; Levchenko, A. Self-organization in high-density bacterial colonies: Efficient crowd control. *PLoS. Biol.* **2007**, *5*, 2614-2623.
- 11. Renner, L. D.; Weibel, D. B. Physicochemical regulation of biofilm formation. *MRS Bull.* **2011**, *36*, 347-355.
- 12. Rzhepishevska, O.; Limanska, N.; Galkin, M.; Lacoma, A.; Lundquist, M.; Sokol, D.; Hakobyan, S.; Sjostedt, A.; Prat, C.; Ramstedt, M. Characterization of clinically relevant

- model bacterial strains of Pseudomonas aeruginosa for anti-biofilm testing of materials. *Acta Biomater.* **2018**, *76*, 99-107.
- 13. Artyushkova, K.; Cornejo, J. A.; Ista, L. K.; Babanova, S.; Santoro, C.; Atanassov, P.; Schuler, A. J. Relationship between surface chemistry, biofilm structure, and electron transfer in Shewanella anodes. *Biointerphases* **2015**, *10*, 019013.
- 14. Gu, H.; Hou, S. Y.; Yongyat, C.; De Tore, S.; Ren, D. C. Patterned Biofilm Formation Reveals a Mechanism for Structural Heterogeneity in Bacterial Biofilms. *Langmuir* **2013**, *29*, 11145-11153.
- 15. Ploux, L.; Beckendorff, S.; Nardin, M.; Neunlist, S. Quantitative and morphological analysis of biofilm formation on self-assembled monolayers. *Colloid Surf. B-Biointerfaces* **2007**, *57*, 174-181.
- 16. Korea, C. G.; Ghigo, J. M.; Beloin, C. The sweet connection: Solving the riddle of multiple sugar-binding fimbrial adhesins in Escherichia coli. *Bioessays* **2011**, *33*, 300-311.
- 17. Thomas, W. E.; Nilsson, L. M.; Forero, M.; Sokurenko, E. V.; Vogel, V. Shear-dependent 'stick-and-roll' adhesion of type 1 fimbriated Escherichia coli. *Mol. Microbiol.* **2004**, *53*, 1545-1557.
- 18. Thomas, W. E.; Trintchina, E.; Forero, M.; Vogel, V.; Sokurenko, E. V. Bacterial adhesion to target cells enhanced by shear force. *Cell* **2002**, *109*, 913-923.
- 19. Bennett, R. R.; Lee, C. K.; De Anda, J.; Nealson, K. H.; Yildiz, F. H.; O'Toole, G. A.; Wong, G. C. L.; Golestanian, R. Species-dependent hydrodynamics of flagellum-tethered bacteria in early biofilm development. *J. R. Soc. Interface* **2016**, *13*, 20150966.
- 20. de Anda, J.; Lee, E. Y.; Lee, C. K.; Bennett, R. R.; Ji, X.; Soltani, S.; Harrison, M. C.; Baker, A. E.; Luo, Y.; Chou, T.; O'Toole, G. A.; Armani, A. M.; Golestanian, R.; Wong, G. C. L. High-Speed "4D" Computational Microscopy of Bacterial Surface Motility. *ACS Nano* **2017**, *11*, 9340-9351.
- 21. Utada, A. S.; Bennett, R. R.; Fong, J. C. N.; Gibiansky, M. L.; Yildiz, F. H.; Golestanian, R.; Wong, G. C. L. Vibrio cholerae use pili and flagella synergistically to effect motility switching and conditional surface attachment. *Nat. Commun.* **2014**, *5*, 4913.
- 22. Sharma, S.; Conrad, J. C. Attachment from Flow of Escherichia coli Bacteria onto Silanized Glass Substrates. *Langmuir* **2014**, *30*, 11147-11155.
- 23. Vissers, T.; Brown, A. T.; Koumakis, N.; Dawson, A.; Hermes, M.; Schwarz-Linek, J.; Schofield, A. B.; French, J. M.; Koutsos, V.; Arlt, J.; Martinez, V. A.; Poon, W. C. K. Bacteria as living patchy colloids: Phenotypic heterogeneity in surface adhesion. *Sci. Adv.* **2018**, *4*, eaao1170

- 24. Agladze, K.; Wang, X.; Romeo, T. Spatial periodicity of Escherichia coli K-12 biofilm microstructure initiates during a reversible, polar attachment phase of development and requires the polysaccharide adhesin PGA. *J. Bacteriol.* **2005**, *187*, 8237-8246.
- 25. Berne, C.; Ducret, A.; Hardy, G. G.; Brun, Y. V. Adhesins Involved in Attachment to Abiotic Surfaces by Gram-Negative Bacteria. *Microbiol. Spectr.* **2015**, *3*, MB-0018-2015.
- 26. Berne, C.; Ellison, C. K.; Ducret, A.; Brun, Y. V. Bacterial adhesion at the single-cell level. *Nat. Rev. Microbiol.* **2018**, *16*, 616-627.
- 27. Jones, J. F.; Velegol, D. Laser trap studies of end-on E-coli adhesion to glass. *Colloid Surf. B-Biointerfaces* **2006**, *50*, 66-71.
- 28. Fei, C. Y.; Mao, S.; Yan, J.; Alert, R.; Stone, H. A.; Bassler, B. L.; Wingreen, N. S.; Kosmrlj, A. Nonuniform growth and surface friction determine bacterial biofilm morphology on soft substrates. *Proc. Natl. Acad. Sci. U. S. A.* **2020**, *117*, 7622-7632.
- 29. Volfson, D.; Cookson, S.; Hasty, J.; Tsimring, L. S. Biomechanical ordering of dense cell populations. *Proc. Natl. Acad. Sci. U. S. A.* **2008**, *105*, 15346-15351.
- 30. Duvernoy, M. C.; Mora, T.; Ardre, M.; Croquette, V.; Bensimon, D.; Quilliet, C.; Ghigo, J. M.; Balland, M.; Beloin, C.; Lecuyer, S.; Desprat, N. Asymmetric adhesion of rod-shaped bacteria controls microcolony morphogenesis. *Nat. Commun.* **2018**, *9*, 1120.
- 31. Carniello, V.; Peterson, B. W.; van der Mei, H. C.; Busscher, H. J. Physico-chemistry from initial bacterial adhesion to surface-programmed biofilm growth. *Adv. Colloid Interface Sci.* **2018**, *261*, 1-14.
- 32. Persat, A.; Nadell, C. D.; Kim, M. K.; Ingremeau, F.; Siryaporn, A.; Drescher, K.; Wingreen, N. S.; Bassler, B. L.; Gitai, Z.; Stone, H. A. The Mechanical World of Bacteria. *Cell* **2015**, *161*, 988-997.
- 33. Redman, J. A.; Walker, S. L.; Elimelech, M. Bacterial adhesion and transport in porous media: Role of the secondary energy minimum. *Environ. Sci. Technol.* **2004**, *38*, 1777-1785.
- 34. Chen, G. X.; Hong, Y. S.; Walker, S. L. Colloidal and Bacterial Deposition: Role of Gravity. *Langmuir* **2010**, *26*, 314-319.
- 35. McLean, R. J. C.; Cassanto, J. M.; Barnes, M. B.; Koo, J. H. Bacterial biofilm formation under microgravity conditions. *FEMS Microbiol. Lett.* **2001**, *195*, 115-119.
- 36. Kaya, T.; Koser, H. Characterization of Hydrodynamic Surface Interactions of Escherichia coli Cell Bodies in Shear Flow. *Phys. Rev. Lett.* **2009**, *103*.

- 37. Shave, M. K. Ph. D. Thesis, University of Massachusetts at Amherst, Interfacial Interactions and Dynamic Adhesion of Synthetic and Living Colloids in Flow. **2019**, 76.
- 38. https://onlinelibrary.wiley.com/doi/pdf/10.1111/mmi.13264.
- 39. Gon, S.; Bendersky, M.; Ross, J. L.; Santore, M. M. Manipulating Protein Adsorption using a Patchy Protein-Resistant Brush. *Langmuir* **2010**, *26*, 12147-12154.
- 40. Hansupalak, N.; Santore, M. M. Polyelectrolyte desorption and exchange dynamics near the sharp adsorption transition: Weakly charged chains. *Macromolecules* **2004**, *37*, 1621-1629.
- 41. Gon, S.; Fang, B.; Santore, M. M. Interaction of Cationic Proteins and Polypeptides with Biocompatible Cationically-Anchored PEG Brushes. *Macromolecules* **2011**, *44*, 8161-8168.
- 42. Shave, M. K.; Kalasin, S.; Ying, E.; Santore, M. M. Nanoscale Functionalized Particles with Rotation-Controlled Capture in Shear Flow. *ACS Appl. Mater. Interfaces* **2018**, *10*, 29058-29068.
- 43. Kalasin, S.; Browne, E. P.; Arcaro, K. F.; Santore, M. M. Surfaces that Adhesively Discriminate Breast Epithelial Cell Lines and Lymphocytes in Buffer and Human Breast Milk. *ACS Appl. Mater. Interfaces* **2019**, *11*, 16347-16356.
- 44. Fang, B.; Jiang, Y.; Rotello, V. M.; Nusslein, K.; Santore, M. M. Easy Come Easy Go: Surfaces Containing Immobilized Nanoparticles or Isolated Polycation Chains Facilitate Removal of Captured Staphylococcus aureus by Retarding Bacterial Bond Maturation. *ACS Nano* **2014**, *8*, 1180-1190.
- 45. Van Rossum, G.; Drake, F. L., *Python 3 Reference Manual*. CreateSpace: Scotts Valley, CA, 2009.
- 46. Harris, L. K.; Theriot, J. A. Relative Rates of Surface and Volume Synthesis Set Bacterial Cell Size. *Cell* **2016**, *165*, 1479-1492.
- 47. Hashimoto, M.; Ichimura, T.; Mizoguchi, H.; Tanaka, K.; Fujimitsu, K.; Keyamura, K.; Ote, T.; Yamakawa, T.; Yamazaki, Y.; Mori, H.; Katayama, T.; Kato, J. Cell size and nucleoid organization of engineered Escherichia coli cells with a reduced genome. *Mol. Microbiol.* **2005**, *55*, 137-149.
- 48. Young, K. D., Bacterial Shape: Two-Dimensional Questions and Possibilities. In *Annual Review of Microbiology, Vol 64, 2010*, Gottesman, S.; Harwood, C. S., Eds. 2010; Vol. 64, pp 223-240.

- 49. Shave, M. K.; Balciunaite, A.; Xu, Z.; Santore, M. M. Rapid Electrostatic Capture of Rod-Shaped Particles on Planar Surfaces: Standing up to Shear. *Langmuir* **2019**, *35*, 13070-13077.
- 50. Jeffery, G. B. The motion of ellipsoidal particles in a viscous fluid. *Proc. R. soc. Lond. Ser. A-Contain. Pap. Math. Phys. Character* **1922**, *102*, 161-179.
- 51. Kalasin, S.; Santore, M. M. Hydrodynamic crossover in dynamic microparticle adhesion on surfaces of controlled nanoscale heterogeneity. *Langmuir* **2008**, *24*, 4435-4438.
- 52. Kalasin, S.; Santore, M. M. Engineering Nanoscale Surface Features to Sustain Microparticle Rolling in Flow. *ACS Nano* **2015**, *9*, 4706-4716.
- 53. Tomotika, S.; Aoi, T. The Steadu Flow of a Viscous FLuid Past an Elliptic Cylinder adn a Flat Plate at Small Reynolds Numbers *Q. J. Mech. Appl. Math.* **1953**, *6*, 290-312.
- 54. Chao, Y. Q.; Zhang, T. Probing Roles of Lipopolysaccharide, Type 1 Fimbria, and Colanic Acid in the Attachment of Escherichia coli Strains on Inert Surfaces. *Langmuir* **2011**, *27*, 11545-11553.
- 55. Strauss, J.; Burnham, N. A.; Camesano, T. A. Atomic force microscopy study of the role of LPS O-antigen on adhesion of E. coli. *J. Mol. Recognit.* **2009**, *22*, 347-355.

TOC graphic:

